Zero Sound Modes in the AdS/CFT Correspondence

by

Thomas Roxlo

Submitted to the Department of Physics
in partial fulfillment of the requirements for the degree of

Bachelor of Science in Physics

at the

MASSACHUSETTS INSTITUTE OF TECHNOLOGY

June 2012

Author .....
Department of Physics
May 11, 2012

Certified by.....
.....
Hong Liu
Professor of Physics
Thesis Supervisor

Accepted by .....
Nergis Mavalvala
Professor, Senior Thesis Coordinator, Department of Physics

Zero Sound Modes in the AdS/CFT Correspondence

by

Thomas Roxlo

Submitted to the Department of Physics
on May 11, 2012, in partial fulfillment of the
requirements for the degree of
Bachelor of Science in Physics

Abstract

We examine the effects of zero sound wave excitations of charged fermion species living around the charged black hole of an AdS/CFT spacetime. In particular, we show that these bulk modes cause corresponding singularities in the correlation functions of boundary gauge fields. Possible implications for the study of non-Fermi liquids are discussed.

Thesis Supervisor: Hong Liu
Title: Professor of Physics

Acknowledgments

I would like to thank my thesis advisor Professor Hong Liu for his clear explanations and valuable comments.

Contents

Chapter 1

Introduction

Gauge/gravity duality [3, 4, 5] has in recent years become one of the most important tools for investigating the behavior of strongly coupled field theories and various classes of non-Fermi liquids that elude description by other methods. In such models, the properties of a d-dimensional conformal field theory (CFT) with a global U(1) symmetry are examined through the properties of its $d+1$-dimensional AdS gravity dual (for examples, see [6], [7]). The classic example of a theory to which this method has been applied is $\mathcal{N}=4$ super-Yang-Mills (SYM) theory in $d=4$ [8], but many other theories can be studied. Thus, a wide range of systems can be evaluated in this manner, from the quark-gluon plasma created in highly relativistic collisions at accelerators like the Relativistic Heavy Ion Collider (RHIC) and the Large Hadron Collider (LHC) to the low temperature behavior of metals and other substances.

Our understanding of low temperature metals and liquids has been dominated by Landau's Fermi liquid theory for over fifty years. This theory describes the behavior of interacting fermion systems in terms of quasiparticle excitations about the Fermi surface. In doing so, it provides simple ways to understand the low temperature properties of the system, and has been extremely successful in describing the behavior of most observed metallic states, from liquid ^3He to heavy fermions in rare earth compounds.

However, in recent times a number of metallic compounds have been discovered whose low-temperature thermodynamic properties differ significantly from the pre-

dictions of Fermi liquid theory [9, 10]. For example, an understanding of the strange metal phase of the high T_c cuprates is considered essential for a description of the mechanism for high T_c superconductivity, but has resisted all theoretical attempts for more than twenty years. While photoemission probes on the strange metal phase do reveal a Fermi surface, anomalous effects such as the "marginal Fermi liquid" [11] form of the spectral function and linear-T resistivity seem to suggest that the quasiparticle description no longer applies to its low energy excitations near the Fermi surface. Other so-called non-Fermi liquids exhibit similar (and sometimes different) anomalous behavior.

Thus, to describe these systems, a low energy theory exhibiting a Fermi surface but no quasiparticles is necessary [12, 13]. AdS/CFT techniques have recently been used to describe a type of non-Fermi liquid [14, 15] which contain low energy excitations governed by a nontrivial infrared (IR) fixed point with nonanalytic scaling in the time direction. The behavior of the low energy excitations about the Fermi surface is governed by the scaling dimension ν of the fermionic operator in the IR fixed point. For $\nu > \frac{1}{2}$ there exists a Fermi surface with well-defined quasiparticles but a scaling energy generally different from that of the Fermi liquid; for $\nu < \frac{1}{2}$ there is a Fermi surface without quasiparticles. For $\nu = \frac{1}{2}$, one finds the marginal Fermi liquid, which can be used to describe the strange metal phase of cuprates.

In this paper, we evaluate the effect on the boundary theory of zero sound excitations in the gravitational bulk. Zero sound waves, originally predicted by Landau in 1957 [16, 17], are propagating distortions of the Fermi surface at low temperatures. They are distinct from normal sound waves because they do not represent changes in density, but rather oscillations of the entire Fermi surface which change its shape but not its size and are restored by attractive interactions between the quasiparticles. Since such modes are present in fermionic theories with quite general interactions, they should be present in the fermion species inhabiting the bulk representation of most AdS/CFT theories. Thus, the duals of these modes in their boundary theories may describe interesting features of non-Fermi liquids or other theories of importance. We shall explicitly calculate the quantity corresponding to zero sound fluctuations in

the bulk in the simplest case of constant $\lambda\psi^4$ fermionic interaction, and show that a pole results in the correlation functions of gauge fields living on the boundary. This shall be done by summing over "ladder diagrams" in the bulk theory. We shall argue that similar results will occur in theories with more complex interactions.

The organization of the paper is as follows. In Chapter 2, we will discuss the Landau theory of Fermi liquids, and derive results for zero sound excitations in flat space. In Chapter 3, we will outline the AdS/CFT correspondence, and describe the geometry of the charged black hole that inhabits its bulk. In Chapter 4, we will compute the 1-loop contribution to the boundary gauge correlator, drawing from the discussion in [1]. Finally, in Chapter 5, we will evaluate the sum of the ladder diagrams, and derive the expression governing the corresponding poles of the boundary Green's function.

Chapter 2

Fermi Liquids and Zero Sound Waves

A system of interacting spin $\frac{1}{2}$ Fermi particles is described by Landau's theory of the Fermi liquid[2]. The theory is based on the assumption that the excitation spectrum of the liquid follows the same principles as that of a Fermi gas. That is, in the ground state of a Fermi gas at $T = 0$, the particles occupy all quantum states with momentum less than or equal to some limiting value p_F, the *Fermi momentum*, with

$$p_F = \left(\frac{3\pi^2 N}{V}\right)^{1/3} \tag{2.1}$$

The occupied states then form the *Fermi sphere*, with the boundary between occupied and unoccupied states referred to as the *Fermi surface*. Excited states are formed by moving one or more particles from their positions below the Fermi surface to open states above it - this creates a state which differs from the ground state by the presence of "particles" with $p > p_F$ and "holes" with $p < p_F$. The particles have energy with respect to the Fermi surface of

$$\epsilon = \frac{p^2}{2m} - \frac{p_F^2}{2m} \approx v(p - p_F), \tag{2.2}$$

with $v = p_F/m$ is the "Fermi velocity," and the holes have energy

$$-\epsilon = \frac{p_F^2}{2m} - \frac{p^2}{2m} \approx v(p_F - p), \tag{2.3}$$

The theory of the Fermi liquid states that even in interacting fermionic systems this basic principle still holds: the low energy excitations of the liquid still take the form of particles and holes which appear and disappear in pairs - these basic units of excitation are referred to as quasiparticles. Further, the location of the Fermi surface depends on the fermion density in the same way as in the Fermi gas. However, due to interactions between the fermions, the excitation spectrum of a Fermi liquid can be quite complicated, leading to complex behaviors such as superfluidity. Since the fermions can interact with each other, the quasiparticles are not fully stable states, but can decay into other quasiparticles of lower energy. The probability of decay increases with the energy of the excitation. Thus, it makes sense to talk about elementary excitations of quasiparticle states only very near the Fermi surface. However, near the surface, there can often exist long-lived, stable, propagating states.

The propagation of sound waves in a Fermi liquid has several interesting features not found in Bose liquids. In particular, at ordinary temperatures sound behaves simply according to ordinary hydrodynamics, with attenuation proportional to the time τ between collisions. As the temperature decreases, the collision time increases as T^{-2}, and when τ reaches the order of ω^-1, where ω is the frequency of the wave, sound ceases to propagate at all. However, Landau predicted that when the temperature is lowered still further sound will eventually be able to propagate again, albeit generally with a different velocity. This phenomenon is known as "zero sound."

Zero sound waves cannot be described as simple waves of compression and rarefaction - they are not disturbances of density as are ordinary sound waves. Instead, they represent oscillating distortions of the Fermi surface that change its shape but not its size (see Figure 2-1). We will now derive the equations governing zero sound.

The low temperature energy distribution of the quasiparticles in momentum space

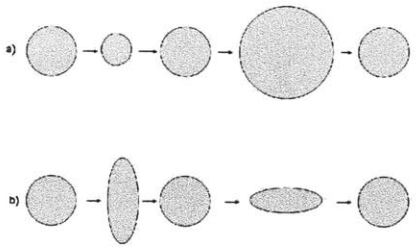

Figure 2-1: (Exaggerated) possible oscillations of the Fermi surface in a) ordinary and b) zero sound waves.

can be represented perturbatively as

$$\epsilon(\boldsymbol{p},\boldsymbol{\sigma}) = \epsilon^{(0)}(\boldsymbol{p},\boldsymbol{\sigma}) + \delta\epsilon(\boldsymbol{p},\boldsymbol{\sigma}), \tag{2.4}$$

where $\epsilon^{(0)}$ is the equilibrium energy and $\boldsymbol{\sigma}$ refers to the spin state of the particle. We can write $\delta\epsilon$ in terms of generalized interactions with the surrounding particles as follows

$$\delta\epsilon(\boldsymbol{p},\boldsymbol{\sigma}) = \sum_{\boldsymbol{\sigma}'} \int f(\boldsymbol{p},\boldsymbol{\sigma};\boldsymbol{p}',\boldsymbol{\sigma}')\delta n(\boldsymbol{p}',\boldsymbol{\sigma}')\frac{d\boldsymbol{p}'}{(2\pi)^3} \tag{2.5}$$

where $f(\boldsymbol{p},\boldsymbol{\sigma};\boldsymbol{p}',\boldsymbol{\sigma}')$ is a function corresponding to the interaction between two quasi-particles with states $(\boldsymbol{p},\boldsymbol{\sigma})$ and $(\boldsymbol{p}',\boldsymbol{\sigma}')$, and $n = n^{(0)} + \delta n$ is the number density of the system. f is in essence the interaction potential, and characterizes the long-distance interactions of the particles.

To study the propagation of sound, we now turn to the Boltzmann transport equation

$$\frac{\partial n}{\partial t} + \nabla_{\boldsymbol{r}} n \cdot \nabla_{\boldsymbol{p}} \epsilon - \nabla_{\boldsymbol{p}} n \cdot \nabla_{\boldsymbol{r}} \epsilon = I(n) \tag{2.6}$$

where $I(n)$ is the collision integral. Note that this can also be written in the perhaps

more familiar form

$$\frac{\partial n}{\partial t} + \nabla_{\boldsymbol{r}} n \cdot \frac{\boldsymbol{p}}{m} + \nabla_{\boldsymbol{p}} n \cdot \boldsymbol{F} = \left.\frac{\partial n}{\partial t}\right|_{coll}, \tag{2.7}$$

with $\boldsymbol{F}$ the force field experienced by the particles, since $\nabla_{\boldsymbol{p}}\epsilon = \nabla_{\boldsymbol{p}}\left(\frac{p^2}{2m}\right) = \frac{\boldsymbol{p}}{m}$ and $\boldsymbol{F} = -\nabla_{\boldsymbol{r}}\epsilon$. Now let us assume that our disturbance takes the form of a propagating wave, so

$$\delta n \propto e^{i(\boldsymbol{k}\cdot\boldsymbol{r}-\omega t)} \tag{2.8}$$

In the low temperature limit, the time between collisions τ is very large. Since the collision integral $I(n)$ is of order $\delta n/\tau$, it is negligible compared to $\frac{\partial n}{\partial t}$ in this limit. Since from equation 2.5 we have

$$\nabla_{\boldsymbol{r}}\epsilon = \sum_{\sigma'}\int f \nabla_{\boldsymbol{r}}\delta n' \frac{d\boldsymbol{p}'}{(2\pi)^3}, \tag{2.9}$$

equation 2.6 takes the form

$$(\boldsymbol{v}\cdot\boldsymbol{k}-\omega)\delta n - (\boldsymbol{v}\cdot\boldsymbol{k})\frac{\partial n^{(0)}}{\partial\epsilon}\sum_{\sigma'}\int f\delta n' \frac{d\boldsymbol{p}'}{(2\pi)^3} = 0 \tag{2.10}$$

using $\nabla_{\boldsymbol{p}}\epsilon = \boldsymbol{v}$ and $\nabla_{\boldsymbol{p}} n = \frac{\partial n}{\partial\epsilon}\nabla_{\boldsymbol{p}}\epsilon \approx \frac{\partial n^{(0)}}{\partial\epsilon}\boldsymbol{v}$. If we now define ν such that

$$\delta n = \frac{\partial n^{(0)}}{\partial\epsilon}\nu, \tag{2.11}$$

this becomes

$$(\boldsymbol{v}\cdot\boldsymbol{k}-\omega)\nu + (\boldsymbol{v}\cdot\boldsymbol{k})\frac{1}{2}\sum_{\sigma'}\int F(\chi)\nu' \frac{d\Omega'}{4\pi} = 0 \tag{2.12}$$

where $F = f\frac{p_F m}{\pi^2}$, since $\frac{\partial n^{(0)}}{\partial\epsilon} \approx -\delta(\epsilon-\mu)$, with μ the chemical potential. Then, taking $\boldsymbol{k}$ to be the polar axis and denoting the velocity of wave propagation as $\tilde{u} = \omega/k$,

equation 2.12 becomes

$$(s - \cos\theta)\nu(\theta, \phi, \boldsymbol{\sigma}) = \cos\theta \frac{1}{2} \sum_{\sigma'} \int F(\chi)\nu(\theta', \phi', \boldsymbol{\sigma}') \frac{d\Omega}{4\pi} \tag{2.13}$$

with $s = \tilde{u}/v$. This equation illustrates the essential difference between ordinary and zero sound: in the latter, the Fermi surface does not remain spherical, but acquires some changing angular dependence. In ordinary sound, of course, the radius of the Fermi sphere may grow or shrink, and its center may oscillate about $\boldsymbol{p} = 0$, but its shape remains the same. In zero sound, the distortion of the Fermi surface is governed by the function ν in equation 2.13.

It is interesting to consider the simplest case, of interactions described by a constant function $F(\chi) = \Phi$. From equation 2.13 we see that

$$\nu = \text{const} \cdot \frac{\cos\theta}{s - \cos\theta} e^{i(\boldsymbol{k}\cdot\boldsymbol{r} - \omega t)}. \tag{2.14}$$

Substituting this ansatz back into 2.13 and integrating, we find an equation for the propagation speed of the zero sound waves:

$$\frac{s}{2} \ln \frac{s+1}{s-1} - 1 = \frac{1}{\Phi} \tag{2.15}$$

We see that if s is real (i.e., the waves are undamped), then s must be larger than 1. This means that $\tilde{u} > v$, for any Φ. Also, the speed of ordinary sound in a weakly non-ideal Fermi gas is given by $u \approx \frac{v}{\sqrt{3}}$, so the speed of zero sound waves can exceed that of normal sound by a factor of $\sqrt{3}$ or more.

2.1 Calculation of zero sound pole in flat space via ladder diagrams

In this section, we will show how the equations of zero sound can be derived from quantum field theory in the case of $\lambda\psi^4$ interactions between the fermions, ie, for a

system with the action

$$S = \int d^4x \left(\bar{\psi}(\partial\!\!\!/ - m)\psi + \lambda\bar{\psi}\psi\bar{\psi}\psi\right) \tag{2.16}$$

The one-particle Green's function for the quasiparticles is given by

$$G(x, x') = -i < T(\tilde{\psi}(x)\tilde{\psi}^\dagger(x')) >, \tag{2.17}$$

where $\tilde{\psi}$ represents the wavefunction of the *quasiparticles* in the Heisenberg representation and is given by

$$\tilde{\psi}(\boldsymbol{r}, t) = \frac{1}{\sqrt{V}} \sum_{\boldsymbol{p}} a_p e^{i[\boldsymbol{p}\cdot\boldsymbol{r} - \epsilon^{(0)}(\boldsymbol{p})t]} \tag{2.18}$$

with a_p the appropriate creation operator. Assuming the system is homogeneous and isotropic, we can substitute 2.18 into 2.17 to obtain the free-field correlator, noting that in the ground state all levels with $|\boldsymbol{p}| < p_0$ are occupied and those with $|\boldsymbol{p}| > p_0$ are empty.

$$G^{(0)}(x) = -\frac{i}{V} \sum_{\boldsymbol{p}} e^{i[\boldsymbol{p}\cdot\boldsymbol{r} - \epsilon^{(0)}(\boldsymbol{p})t]} \begin{cases} 1 - n_{\boldsymbol{p}} & \text{for } t > 0, \\ -n_{\boldsymbol{p}} & \text{for } t < 0, \end{cases} \tag{2.19}$$

where

$$n_{\boldsymbol{p}} = a^\dagger_{\boldsymbol{p}} a_{\boldsymbol{p}} = \begin{cases} 1 & \text{for } |\boldsymbol{p}| < p_0, \\ 0 & \text{for } |\boldsymbol{p}| > p_0. \end{cases} \tag{2.20}$$

We can then move to momentum space as follows

$$G(x - x') = \int G(\boldsymbol{p}, \omega) e^{i[\boldsymbol{p}\cdot(\boldsymbol{r} - \boldsymbol{r}') - \omega(t - t')]} \frac{d^4p}{(2\pi)^4} \tag{2.21}$$

where

$$G^{(0)}(\boldsymbol{p},\omega) = -i\left\{\theta(|\boldsymbol{p}|-p_0)\int_0^\infty e^{i[\omega-\epsilon^{(0)}(\boldsymbol{p})]t}dt - \theta(p_0-|\boldsymbol{p}|)\int_0^\infty e^{-i[\omega-\epsilon^{(0)}(\boldsymbol{p})]t}dt\right\}, \tag{2.22}$$

with θ the Heaviside step function. Now, integrals of the form $\int_0^\infty e^{ist}dt$ can be expressed via the limit

$$\lim_{\delta\to+0}\int_0^\infty e^{isnt-\delta t}dt = i\lim_{\delta\to+0}\frac{1}{s+i\delta}. \tag{2.23}$$

Thus, we find that

$$\begin{aligned} G^{(0)}(\boldsymbol{p},\omega) &= \frac{\theta(|\boldsymbol{p}|-p_0)}{\omega-\epsilon^{(0)}(\boldsymbol{p})+i\delta} + \frac{\theta(p_0-|\boldsymbol{p}|)}{\omega-\epsilon^{(0)}(\boldsymbol{p})-i\delta} \\ &= \frac{1}{\omega-\epsilon^{(0)}(\boldsymbol{p})+i\delta\mathrm{sgn}(|\boldsymbol{p}|-p_0)}. \end{aligned} \tag{2.24}$$

The change of sign in the denominator comes from the time-ordering of the ψs, and characterizes the way the poles are integrated over in the Feynman propagator. Near the Fermi surface, the G-function can then be expressed to lowest order as

$$G(\boldsymbol{p},\omega) = \frac{a}{\omega - v(|\boldsymbol{p}|-p_0)+i\delta\mathrm{sgn}(|\boldsymbol{p}|-p_0)} \tag{2.25}$$

where $|\boldsymbol{p}| \approx p_0$, $\omega \approx 0$, we take the limit $\delta \to 0$, and a is a positive constant. v is the Fermi velocity, the velocity of excitations at the Fermi surface, and is equal to p_0/m^*, where m^* is the effective mass of the quasiparticles.

Zero sound modes can be seen by examining the properties of the effective 4-vertex $\Gamma(p_1,p_2;p_1+k,p_2-k) \equiv \Gamma(p_1,p_2;k)$, where the momentum transfer $k = (\omega,\boldsymbol{k})$ is a small 4-vector with $|\boldsymbol{k}| \ll p_0$, $|\omega| \ll \mu$. The three possible 1-loop diagrams for this vertex are shown in Figure 2-2. While diagrams (a) and (b) are well-behaved for $k = 0$, the poles of the two Green's functions converge in diagram (c). As we shall see, this causes singularities to appear in Γ. If we denote by $\Gamma^{(1)}$ the set of all diagrams which do not contain singularities in the form of $G(q)G(q+k)$ lines, we can see that

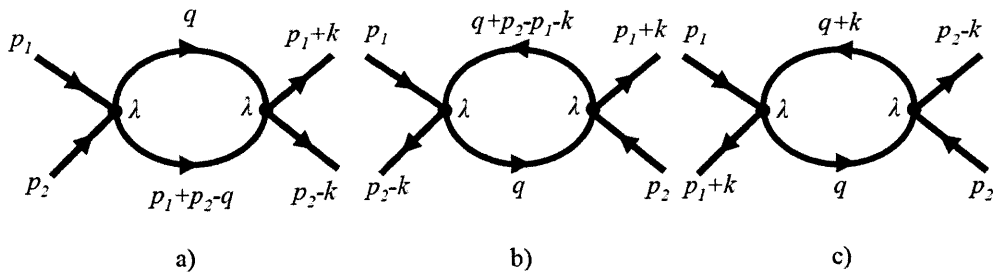

Figure 2-2: 1-loop diagrams making up the vertex Γ.

the exact Γ is obtained by summing over the "ladder diagrams" shown in Figure 2-3. To first order, this sum can be computed by approximating $\Gamma^{(1)} = \lambda$. We will now

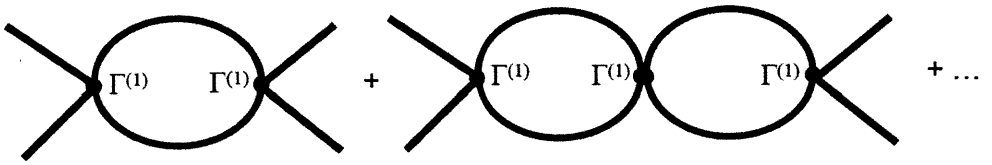

Figure 2-3: Series of ladder diagrams making up Γ.

perform this calculation. The 1-loop diagram (c) of Figure 2-2 gives a contribution to the vertex of

$$\Gamma(p_1, p_2; k) = -i\lambda^2 \int \frac{d^d q}{(2\pi)^d} \mathrm{tr}[G(q+k)G(q)] \tag{2.26}$$

Each additional loop adds a factor of the form

$$\Sigma = -i\lambda \int \frac{d^d q}{(2\pi)^d} \mathrm{tr}[G(q+k)G(q)], \tag{2.27}$$

so the sum of all ladder diagrams can be expressed as the sum of a geometric series (including the tree level diagram):

$$\Gamma(p_1, p_2; k) = \frac{\lambda}{1 - \Sigma(k)} \tag{2.28}$$

To evaluate the integral in Σ, we note that since the arguments of the G-functions are

very close together, we can divide the integral into a part due to the pole structure of the integrand and a part due to a "distant" integration in which k is set to 0. Basic contour integration tells us that the poles will only contribute if they are located on opposite sides of the real axis. From Equation 2.25, we see that this requires that $|\boldsymbol{q}| < p_0$, $|\boldsymbol{q}+\boldsymbol{k}| > p_0$ or $|\boldsymbol{q}| > p_0$, $|\boldsymbol{q}+\boldsymbol{k}| < p_0$. Since k is small, this implies that $|\boldsymbol{q}| \approx p_0$ and $\epsilon \approx 0$, with $q = (\epsilon, \boldsymbol{q})$. Thus, $G(q)G(q+k)$ can be replaced by a term proportional to $\delta(\epsilon)\delta(|\boldsymbol{q}| - p_0)$ in the "near" integral. The integral can be carried out by using Cauchy's integral formula and multiplying by $\boldsymbol{v}\cdot\boldsymbol{k}$ to represent the range of q values for which the poles lie on opposite sides of the real axis, with $\boldsymbol{v}$ a vector directed along $\boldsymbol{q}$ and equal to v in absolute value. This gives us the result

$$\Sigma = -i\lambda \int \frac{d^d q}{(2\pi)^d} \left[\frac{2\pi i a^2}{v} \frac{\boldsymbol{v}\cdot\boldsymbol{k}}{\omega - \boldsymbol{v}\cdot\boldsymbol{k}} \delta(\epsilon)\delta(|\boldsymbol{q}| - p_0) + G(q)^2 \right], \tag{2.29}$$

where the $G(q)^2$ term represents the "distant" integration. From (2.25) we see that the distant integration is just 0, and so (2.28) gives us

$$\Gamma = \frac{\lambda}{1 - \lambda \frac{a^2 p_0^{d-2}}{v(2\pi)^{d-1}} \int d\Omega \frac{\boldsymbol{v}\cdot\boldsymbol{\kappa}}{\omega - \boldsymbol{v}\cdot\boldsymbol{\kappa}}} \tag{2.30}$$

Note that if we define

$$\nu(p_1) = \frac{\boldsymbol{n}\cdot\boldsymbol{k}}{\omega - v\boldsymbol{n}\cdot\boldsymbol{k}} \Gamma(p_1, p_2; k), \tag{2.31}$$

where $\boldsymbol{n}$ is a unit vector directed along $\boldsymbol{p_1}$, Equation 2.30 can be rearranged as

$$\begin{aligned} \Gamma(p_1, p_2; k) &= \lambda + \lambda\Gamma(p_1, p_2; k) \frac{a^2 p_0^{d-2}}{v(2\pi)^{d-1}} \int d\Omega \frac{\boldsymbol{v}\cdot\boldsymbol{k}}{\omega - \boldsymbol{v}\cdot\boldsymbol{k}} \\ (\omega - v\boldsymbol{n}\cdot\boldsymbol{k})\nu(p_1) &= \lambda \boldsymbol{n}\cdot\boldsymbol{k} \frac{a^2 p_0^{d-2}}{(2\pi)^{d-1}} \int d\Omega \nu(q). \end{aligned} \tag{2.32}$$

This equation is identical to Equation 2.12 with $F = \frac{2a^2 p_0^{d-2}}{v(2\pi)^{d-2}}$. Thus, we have demonstrated that the system experiences zero sound waves with a constant interaction form factor.

If we carry out the integration further, we find that

$$\begin{aligned}\Gamma &= \frac{\lambda}{1-\lambda\frac{a^2p_0^{d-2}}{v(2\pi)^{d-1}}\int d\Omega\frac{v\cdot\kappa}{\omega-v\cdot\kappa}} = \frac{\lambda}{1-\lambda\frac{a^2p_0^{d-2}}{v(2\pi)^{d-1}}\int d\Omega\frac{|v||\kappa|\cos\theta}{\omega-|v||\kappa|\cos\theta}} \\ &= \frac{\lambda}{1-\lambda\frac{a^2p_0^{d-2}}{v(2\pi)^{d-1}}S_{d-3}\int_{-1}^{1}d(\cos\theta)\frac{\sin^{d-4}\theta\cos\theta}{\frac{\omega}{|v||\kappa|}-\cos\theta}}\end{aligned} \tag{2.33}$$

Specializing to $d = 4$, we find that

$$\Gamma = \frac{\lambda}{1-\lambda\frac{a^2p_0^2}{v(2\pi)^2}\int_{-1}^{1}dx\frac{x}{\frac{\omega}{|v||\kappa|}-x}} \tag{2.34}$$

This implies that $\Gamma = 0$ for $0 < \omega \leq v|\boldsymbol{k}|$, since the integral in the denominator diverges. For $\omega > v|\boldsymbol{k}|$, the stable undamped modes are given by the singularities of this expression, that is, by the zeroes of the denominator. In this domain, the integral has solution

$$\int_{-1}^{1}\frac{x}{s-x}dx = -2 + s\ln\frac{s+1}{s-1}, \quad \text{with } s = \frac{\omega}{v|\boldsymbol{k}|} \tag{2.35}$$

Then, defining $\Phi = \lambda\frac{2a^2p_0^2}{v(2\pi)^2}$, the singularities of the expression are the solutions to the equation

$$1 - \frac{\Phi}{2}(-2 + s\ln\frac{s+1}{s-1}) = 0 \tag{2.36}$$

$$\frac{s}{2}\ln\frac{s+1}{s-1} - 1 = \frac{1}{\Phi}. \tag{2.37}$$

This is exactly Equation 2.15! Thus, we have derived the equation governing the propagation speed of the zero sound waves, in terms of λ and p_0, and the free fermion propagator.

Chapter 3

AdS/CFT and Black Hole Geometry

The AdS/CFT correspondence[18] is one of the most significant developments of string theory, and, indeed, all of modern physics. It refers to a set of dualities between gauge theories without gravity and gravity theories of one greater dimension, and is thus sometimes referred to as the gauge-gravity correspondence. The original and most famous example, conjectured by Maldacena in 1997[3], is the exact equivalence between type IIB string theory compactified on $AdS_5 \times S^5$ space and four-dimensional $\mathcal{N} = 4$ supersymmetric Yang-Mills theory (here, AdS_5 refers to five-dimensional anti-de Sitter space, and S^5 denotes a five-sphere). Remarkably, these two apparently very different theories have exactly matching symmetry groups. More, in the low energy limit of the gravity side, which corresponds to the large N and $g^2_{YM}N$ limit on the gauge theory side, the equivalence between the two theories has been well tested. It is more difficult to prove the full, general equivalence, but it is thought to be true as well.

One of the most interesting aspects of AdS/CFT is its relation to the holographic principle. The holographic principle originated in the work of Bekenstein and Hawking[19], which showed that the entropy of a black hole is proportional to its surface area via $S = A/4G$, where G is Newton's constant. Since a black hole represents the state of highest entropy for a given volume (adding information-carrying

matter to a region of space will eventually turn it into a black hole, but adding matter to a black hole will just make it bigger), this implies that the maximum information encoded by a region of space in any theory that contains gravity is proportional to its surface area rather than its volume - a tremendously non-intuitive result. This leads to the *holographic principle*, proposed by 't Hooft and formalized by Susskind[20], which states that any volume of space can be described by an encoding on its boundary. The AdS/CFT correspondence is an explicit realization of this principle: a d+1-dimensional bulk gravity theory is equivalent to a d-dimensional gauge theory living on its boundary.

3.1 Black Hole Geometry

In the presence of a finite density state of the boundary CFT_d, the gravity side acquires a charged black hole sitting in d+1-dimensional anti-de Sitter spacetime. Essentially, this is because a finite chemical potential μ in the gauge theory imposes an energy cutoff, which corresponds to a cutoff on the radial direction in the gravity theory. Following [1], we consider the case of a non-zero chemical potential for a $U(1)$ global symmetry. The conserved current J_μ of the boundary global U(1) is dual to a bulk U(1) gauge field A_M, under which the black hole is charged. This results in a non-zero classical background for the electrostatic potential $A_t(r)$.

The action for the vector field A_M in AdS_{d+1} geometry can be written:

$$S = \frac{1}{2\kappa^2}\int d^{d+1}x\sqrt{-g}\left[\mathcal{R} - \frac{d(d-1)}{R^2} - \frac{R^2}{g_F^2}F^{\mu\nu}F_{\mu\nu}\right] \tag{3.1}$$

with the black hole metric

$$\begin{aligned} ds^2 &\equiv -g_{tt}dt^2 + g_{rr}dr^2 + g_{ii}d\vec{x}^2 \\ &= \frac{r^2}{R^2}(-hdt^2 + d\vec{x}^2) + \frac{R^2}{r^2}\frac{dr^2}{h} \end{aligned} \tag{3.2}$$

with

$$h = 1 + \frac{Q^2}{r^{2d-2}} - \frac{M}{r^d}$$
$$A_t = \mu \left(1 - \frac{r_0^{d-2}}{r^{d-2}} \right) \tag{3.3}$$

where Q is the charge of the black hole and M is its mass.

From the resulting equations of motion, one can consider small fluctuations in the gauge field $\delta A_0 \equiv a_0$ and calculate their corresponding effect on the boundary current J_0 in the form of a bulk-to-boundary propagator $K_A(r;\Omega)$. This is necessary to explicitly compute the boundary current correlator which occupies our discussion. However, as we will see, the explicit form of K_A is not necessary for the examination of the zero sound modes, and so we will not derive it here. For the interested reader, it is calculated in detail in [1].

Chapter 4

1-loop diagram

We wish to compute the contribution to the correlation function of the time component of the gauge field from a series of loop diagrams similar to those described in Chapter 2. In general, loop diagrams in black hole geometries are quite tricky. This is because of issues integrating over the volume of the black hole, as well as dealing with diagrams such as that in figure 4-1, where a loop is cut in half by the horizon. A standard strategy is to compute the correlation function in Euclidean signature,

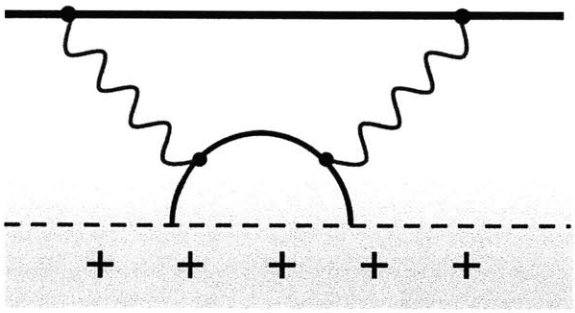

Figure 4-1: Diagrams in which the fermion loop goes into the horizon, corresponding to the decay of particles falling into the black hole[1].

which avoids these problems, and then obtain the Lorentzian expression via analytic continuation:

$$G_R(\Omega, \boldsymbol{\kappa}) = G_E(i\Omega_l = \Omega + i\epsilon, \boldsymbol{\kappa}) \tag{4.1}$$

However, this requires a precise understanding of the Euclidean correlation function, which we do not have. Therefore, modelling our work off of [1], we will adopt a hybrid approach: write down an integral expression for $G_E(i\Omega_l, \boldsymbol{\kappa})$ in Euclidean signature, and then perform analytic continuation 4.1 to Lorentzian signature inside the integral. In this section, we will perform this calculation at the 1-loop level, which is very similar to the conductivity calculation performed in [1]. In the next, we will analyze the sum of 2-loop and higher ladder diagrams, and extract from them the zero sound pole.

The 1-loop diagram we wish to evaluate is shown in Figure 4-2. We will neglect

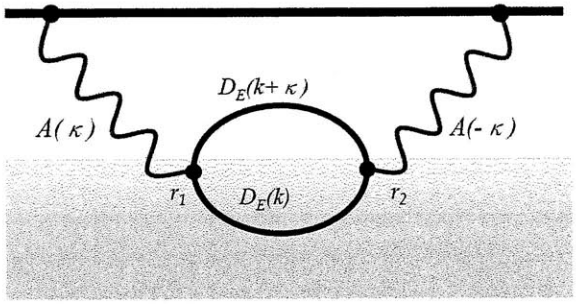

Figure 4-2: 1-loop contribution to the sum of ladder diagrams making up the zero sound excitations.

a number of complications (spinor indices, gauge-graviton mixing, etc) which are unnecessary for the spirit of the calculation. Also, we will omit some details which can be found in [1].

We consider a spinor field living in the spacetime of the charged black hole of (3.2). It is governed by the action

$$S = -\int d^{d+1}x\sqrt{-g}i(\bar{\psi}\Gamma^M\mathcal{D}_M\psi - m\bar{\psi}\psi) \tag{4.2}$$

where $\bar{\psi} = \psi^\dagger\Gamma^{\underline{t}}$ and

$$\mathcal{D}_M = \partial_M + \frac{1}{4}\omega_{abM}\Gamma^{ab} - iqA_M. \tag{4.3}$$

Here $M, N, ...$ are curved space indices, and $a, b, ...$ and underlined indices refer to the

tangent space. That is,

$$\Gamma^M = \Gamma^a e_a^M, \quad \Gamma^r = \sqrt{g^{rr}}\Gamma^{\underline{r}} \tag{4.4}$$

with e_a^M the frame field basis vectors. We consider a small perturbation in the time component of the gauge field, $a_0 \equiv \delta A_0$. The correction to the Dirac action from this perturbation is given by

$$\begin{aligned} \delta S[a_0, \psi] &= -i \int d^{d+1}x \sqrt{-g} \bar{\psi}(-iqa_0\Gamma^t)\psi \\ &= -q \int d^{d+1}x \sqrt{-g} \bar{\psi} a_0 \Gamma^t \psi \end{aligned} \tag{4.5}$$

This can be written in momentum space as

$$\delta S = -T^2 \sum_{\omega_m} \sum_{\Omega_l} \int \frac{d^{d-1}\boldsymbol{k}}{(2\pi)^{d-1}} \int \frac{d^{d-1}\boldsymbol{\kappa}}{(2\pi)^{d-1}} \int dr \sqrt{-g} \bar{\psi}(r; i\omega_m + i\Omega_l, \boldsymbol{k} + \boldsymbol{\kappa}) B(r; i\Omega_l, \boldsymbol{\kappa}) \psi(r; i\omega_m, \boldsymbol{k}) \tag{4.6}$$

where the kernel B contains the dependence of gauge fluctuations as

$$B(r; i\Omega_l, \boldsymbol{\kappa}) = -qa_0(r; i\Omega_l, \boldsymbol{\kappa})\Gamma^t \tag{4.7}$$

In general, if the gauge field under discussion is the field with which the black hole is charged, we must also consider its coupling to the graviton field. This will slightly change the form of B by adding in terms related to the metric fluctuation h_μ^ν. However, this difference is not particularly significant for the characteristics we are interested in (and not necessary for the extraction of zero sound), so we will assume that we are calculating the correlator for a current distinct from the charge of the black hole.

This means that the term in the effective action corresponding to Figure 4-2 is

$$\Gamma[a_0] = -\frac{T^2}{2}\sum_{\omega_m,\Omega_l}\int\frac{d^{d-1}\boldsymbol{k}}{(2\pi)^{d-1}}\frac{d^{d-1}\boldsymbol{\kappa}}{(2\pi)^{d-1}}\int dr_1\sqrt{g(r_1}dr_2\sqrt{g(r_2}$$
$$\times \operatorname{tr}\left(D_E(r_1,r_2;i\omega_m+i\Omega_l,\boldsymbol{k}+\boldsymbol{\kappa})B(r_2;\Omega_l,\boldsymbol{\kappa})D_E(r_2,r_1;i\omega_m,\boldsymbol{\kappa})B(r_1;-\Omega_l,-\boldsymbol{\kappa})\right) \tag{4.8}$$

We can now express B in terms of the momentum space Euclidean boundary-to-bulk propagator, using

$$a_0(r;i\Omega_l,\boldsymbol{\kappa}) = K_A(r;i\Omega_l,\boldsymbol{\kappa})A_0(i\Omega_l,\boldsymbol{\kappa}), \tag{4.9}$$

where A_0 is the source of the boundary conserved current and K_A the propagator that takes the current from the boundary to a point on the interior. Thus, we can define B in a way that explicitly separates its dependence on the boundary current:

$$B(r;i\Omega_l,\boldsymbol{\kappa}) = Q(r;i\Omega_l,\boldsymbol{\kappa})A_0(i\Omega_l,\boldsymbol{\kappa}) \tag{4.10}$$

where Q is a new operator given by

$$Q(r;i\Omega_l,\boldsymbol{\kappa}) = -qK_A(r;i\Omega,\boldsymbol{\kappa})\Gamma^t \tag{4.11}$$

We can extract the correlation function from the effective action (4.8) by taking two functional derivatives with respect to A_0. We find:

$$G_E(i\Omega_l,\boldsymbol{\kappa}) = -T\sum_{i\omega_n}\int\frac{d^{d-1}k}{(2\pi)^{d-1}}dr_1\sqrt{g(r_1)}dr_2\sqrt{g(r_2)}$$
$$\times \operatorname{tr}\left[D_E(r_1,r_2;i\Omega_l+i\omega_n,\boldsymbol{k}+\boldsymbol{\kappa})Q(r_1;i\Omega_l,\boldsymbol{\kappa})D_E(r_2,r_1;i\omega_n,\boldsymbol{k})Q(r_2;-i\Omega_l,-\boldsymbol{\kappa})\right] \tag{4.12}$$

where $D_E(r_1,r_2;i\omega_n,\boldsymbol{k})$ is the Euclidean spinor propagator and with K_A the boundary-to-bulk propagator for the gauge field and Γ^t the 0-th Dirac gamma matrix. We can

perform the Euclidean frequency sum using the spectral representation of the Euclidean Green's function,

$$D_E(r_1, r_2; i\omega_m, \boldsymbol{k}) = \int \frac{d\omega}{(2\pi)} \frac{\rho(r_1, r_2; \omega, \boldsymbol{k})}{i\omega_m - \omega}, \tag{4.13}$$

where $\rho(r_1, r_2; \omega, \boldsymbol{k})$ is the bulk-to-bulk spectral density. As discussed in great detail in [1], $\rho(r_1, r_2; \omega, \boldsymbol{k})$ can be written in terms of the boundary theory spectral density $\rho_B(\omega, \boldsymbol{k})$ as

$$\rho(r_1, r_2; \omega, \boldsymbol{k}) = \psi(r_1; \omega, \boldsymbol{k}) \rho_B(\omega, \boldsymbol{k}) \bar{\psi}(r_2; \omega, \boldsymbol{k}) \tag{4.14}$$

where $\psi(r)$ is the unique normalizable spinor wavefunction solution to the Dirac equation in the Lorentzian black hole geometry. This result is non-trivial and we will not derive it here, but it is extremely important because it means that the bulk-to-bulk spectral density factorizes in the radial direction. This allows us to separate its radial degree of freedom from those in the boundary, and to perform calculations on them separately. As we will see, this makes it possible to compute the loop diagrams we want as though we were performing calculations in the boundary space, with effective vertices determined by integrals over the radial direction.

Substituting 4.13 into 4.12, we can perform the Matsubara frequency summation using the identity

$$T \sum_{\omega_m} \frac{1}{i(\omega_m + \Omega_l) - \omega_1} \frac{1}{i\omega_m - \omega_2} = \pm \frac{f(\omega_1) - f(\omega_2)}{\omega_1 - i\Omega_l - \omega_2} \tag{4.15}$$

with

$$f(\omega) = \frac{1}{e^{\beta\omega} \pm 1} \tag{4.16}$$

Here the Matsubara summation refers to summing over values of $\omega_m = \frac{2\pi m}{\beta}$ with m a half integer for fermions and an integer for bosons (of course, in our discussions we are speaking of fermions) and $\beta = \frac{1}{kT}$. Similarly, $\Omega_l = \frac{2\pi l}{\beta}$. Also, the upper sign is

used for fermions and the lower for bosons.

This leads to the expression for the Green's function, using $\kappa = (i\Omega_l, \boldsymbol{\kappa})$,

$$G_E(\kappa) = -\int \frac{d\omega_1}{2\pi}\frac{d\omega_2}{2\pi}\int \frac{d^{d-1}\boldsymbol{k}}{(2\pi)^{d-1}}\frac{f(\omega_1)-f(\omega_2)}{\omega_1 - i\Omega_l - \omega_2} \times \mathrm{tr}\left[\rho_B(\omega_1, \boldsymbol{k}+\boldsymbol{\kappa})\Lambda(\omega_1,\omega_2,\kappa,\boldsymbol{k})\rho_B(\omega_2,\boldsymbol{k})\Lambda(\omega_2,\omega_1,-\kappa,\boldsymbol{k})\right] \tag{4.17}$$

where

$$\Lambda(\omega_1,\omega_2,i\Omega_l,\boldsymbol{\kappa},\boldsymbol{k}) = \int dr\sqrt{g}\bar{\psi}(r;\omega_1,\boldsymbol{k}+\boldsymbol{\kappa})Q(r;i\Omega_l,\boldsymbol{\kappa})\psi(r;\omega_2,\boldsymbol{k}) \tag{4.18}$$

Here we have absorbed the entire radial dependence into the effective vertex Λ, allowing us to express the Green's function purely in terms of the *boundary* spectral function ρ_B.

We can then obtain the retarded Green function for the currents by analytically continuing $G_E(i\Omega_l, \boldsymbol{\kappa})$ to Lorentzian signature with

$$G_R(\Omega,\boldsymbol{\kappa}) = G_E(i\Omega_l + i\epsilon, \boldsymbol{\kappa}) \tag{4.19}$$

Suppressing the $i\epsilon$ in the function arguments, we find

$$G_R(\Omega,\boldsymbol{\kappa}) = -\int \frac{d\omega_1}{2\pi}\frac{d\omega_2}{2\pi}\int \frac{d^{d-1}\boldsymbol{k}}{(2\pi)^{d-1}}\frac{f(\omega_1)-f(\omega_2)}{\omega_1 - \Omega - \omega_2 - i\epsilon} \times \mathrm{tr}\left[\rho_B(\omega_1, \boldsymbol{k}+\boldsymbol{\kappa})\Lambda(\omega_1,\omega_2,\Omega,\boldsymbol{\kappa},\boldsymbol{k})\rho_B(\omega_2,\boldsymbol{k})\Lambda(\omega_2,\omega_1,\Omega,-\boldsymbol{\kappa},\boldsymbol{k})\right] \tag{4.20}$$

where both $\Lambda(\omega_1,\omega_2,\pm i\Omega_l,\boldsymbol{\kappa},\boldsymbol{k})$ analytically continue to $\Lambda(\omega_1,\omega_2,\Omega,\boldsymbol{\kappa},\boldsymbol{k})$, since $K_A(-i\Omega_l,\boldsymbol{\kappa}) = K_A(i\Omega_l,\boldsymbol{\kappa})$. One can simplify this further by explicitly specifying the form of ρ_B near the Fermi surface and carrying out the integrations, but we will not do this here because this schematic form is sufficient to guide us in our analysis of the 2-loop and higher diagrams. We will wait until our discussion of zero sound modes to delve deeper into the composition of the spectral function.

Chapter 5

Sum of Ladder Diagrams

Suppose now the bulk fermion species has some two-particle interaction characterized by a constant vertex element λ as in Chapter 2. Then the boundary gauge propagator will receive additional corrections arising from intra-fermionic interactions. As we did in the flat space case, we can organize these corrections into a series of ladder diagrams containing "anomalous" fermion loops, where the loops are connected by an effective 4-vertex composed of "non-anomalous" diagrams which can be approximated as λ to first order in the interaction. The difference from the flat space case is that our spacetime is no longer isotropic; the radial direction behaves differently from the others. Thus, we must use the analysis of the last section to package the diagrams in terms of boundary quantities and effective vertices, at which point we can carry out a calculation analogous to that of Chapter 2.

The ladder diagrams we wish to evaluate are shown in Figure 5-1. The contribu-

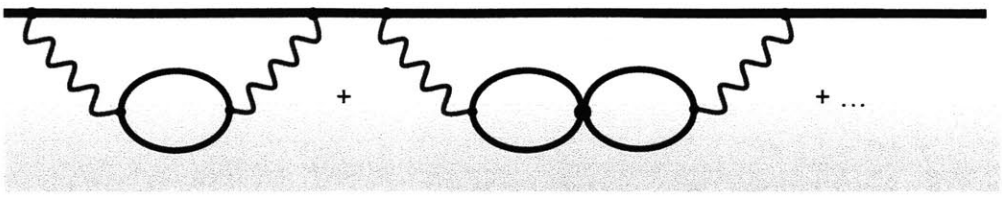

Figure 5-1: Sum of ladder diagrams that make up the first-order contribution to the zero sound pole of the boundary gauge field correlation function.

tion of the 1-loop diagram is given by Equation 4.20. Since the interior 4-vertices do

not depend on momentum, we can separate integrals over the loop momentum in the 2-loop diagram, which gives it the form

$$\begin{aligned} G_R(\Omega,\boldsymbol{\kappa}) = -\lambda \int \frac{d\omega_1}{2\pi}\frac{d\omega_2}{2\pi} \int \frac{d^{d-1}\boldsymbol{k_1}}{(2\pi)^{d-1}} \frac{f(\omega_1)-f(\omega_2)}{\omega_1-\Omega-\omega_2-i\epsilon} \\ \times \int \frac{d\omega_3}{2\pi}\frac{d\omega_4}{2\pi} \int \frac{d^{d-1}\boldsymbol{k_2}}{(2\pi)^{d-1}} \frac{f(\omega_3)-f(\omega_4)}{\omega_3-\Omega-\omega_4-i\epsilon} \\ \times \mathrm{tr}\left[\rho_B(\omega_1,\boldsymbol{k_1}+\boldsymbol{\kappa})\Lambda(\omega_1,\omega_2,\Omega,\boldsymbol{\kappa},\boldsymbol{k_1})\rho_B(\omega_2,\boldsymbol{k_1})\right] \\ \times \int dr\sqrt{g(r)}\bar{\psi}(r;\omega_2,\boldsymbol{k_1})\psi(r;\omega_1,\boldsymbol{k_1}+\boldsymbol{\kappa})\bar{\psi}(r;\omega_4,\boldsymbol{k_2})\psi(r;\omega_3,\boldsymbol{k_2}+\boldsymbol{\kappa}) \\ \times \mathrm{tr}\left[\rho_B(\omega_3,\boldsymbol{k_2}+\boldsymbol{\kappa})\rho_B(\omega_4,\boldsymbol{k_2})\Lambda(\omega_4,\omega_3,\Omega,-\boldsymbol{\kappa},\boldsymbol{k_2})\right] \end{aligned} \tag{5.1}$$

where all terms that depend r, the radial coordinate of the interior point, have been grouped together in a $\bar{\psi}\psi\bar{\psi}\psi$ factor in the middle of the expression. Near the Fermi surface, the wavefunctions can be approximated by their value at the Fermi momentum, and thus ψ can be viewed as roughly constant in ω and k. We see that, in this case, the momentum integrals for each loop separate cleanly. More, as more loops are added to the diagram, they each add only another integral over an "empty" loop, that is, a loop which does not contain a Λ vertex. Thus, the n-loop term of the correlator can be expressed as

$$G(\kappa) = \Xi(\kappa)\chi(\xi(\kappa)\chi)^{n-2}\Xi'(\kappa) \tag{5.2}$$

where

$$\begin{aligned} \Xi(\kappa) &= \int \frac{d\omega_1}{2\pi}\frac{d\omega_2}{2\pi}\frac{f(\omega_1)-f(\omega_2)}{\omega_1-\Omega-\omega_2-i\epsilon}\int \frac{d^{d-1}\boldsymbol{k}}{(2\pi)^{d-1}}\mathrm{tr}\left[\rho_B(\omega_1,\boldsymbol{k}+\boldsymbol{\kappa})\Lambda(\omega_1,\omega_2,\kappa,\boldsymbol{k})\rho_B(\omega_2,\boldsymbol{k})\right] \\ \Xi'(\kappa) &= \int \frac{d\omega_1}{2\pi}\frac{d\omega_2}{2\pi}\frac{f(\omega_1)-f(\omega_2)}{\omega_1-\Omega-\omega_2-i\epsilon}\int \frac{d^{d-1}\boldsymbol{k}}{(2\pi)^{d-1}}\mathrm{tr}\left[\rho_B(\omega_1,\boldsymbol{k}+\boldsymbol{\kappa})\rho_B(\omega_2,\boldsymbol{k})\Lambda(\omega_2,\omega_1,-\kappa,\boldsymbol{k})\right] \\ \chi &= \lambda\int dr\sqrt{g(r)}\bar{\psi}(r)\psi(r)\bar{\psi}(r)\psi(r) \\ \xi(\kappa) &= \int \frac{d\omega_1}{2\pi}\frac{d\omega_2}{2\pi}\frac{f(\omega_1)-f(\omega_2)}{\omega_1-\Omega-\omega_2-i\epsilon}\int \frac{d^{d-1}\boldsymbol{k}}{(2\pi)^{d-1}}\mathrm{tr}\left[\rho_B(\omega_1,\boldsymbol{k}+\boldsymbol{\kappa})\rho_B(\omega_2,\boldsymbol{k})\right] \end{aligned} \tag{5.3}$$

where $\psi(r)$ denotes $\psi(r; 0, \boldsymbol{k_F})$.

Written in this form, we can extract the zero sound singularity by considering the sum of 2-loop and higher diagrams as a geometric series. This sum is given by

$$G(\kappa) = \frac{\Xi(\kappa)\Xi'(\kappa)\chi}{1 - \xi(\kappa)\chi} \tag{5.4}$$

which means that the zero-sound pole occurs at $1 - \xi(\kappa)\chi = 0$.

Near the Fermi surface and near $T = 0$, the bulk fermionic Green's function can be expressed as

$$G^R_{bulk}(\omega, k) = \frac{a}{\omega - v_F(k - k_F) - \Gamma(\omega)}, \tag{5.5}$$

where Γ is the quasiparticle self-energy and represents its decay rate through interactions. In a traditional Landau Fermi liquid, such as the fermion bath in the bulk,

$$\Gamma \sim i\omega^2. \tag{5.6}$$

At low frequency, we can bundle the ω term in the denominator into k_F to get a frequency-dependent Fermi momentum:

$$G^R_{bulk}(\omega, k) = \frac{h_1}{k - k_F(\omega) - \Sigma(\omega)}, \tag{5.7}$$

where $k_F(\omega) = k_F + \frac{1}{v_F}\omega$, $h_1 = -a/v_F$, and $\Sigma = -\Gamma/v_F$.

The spectral function can be obtained from this through

$$\rho_B(\omega, \boldsymbol{k}) = 2\mathrm{Im}G^R_{bulk} = \frac{2h_1 \mathrm{Im}\Sigma(\omega)}{(|\boldsymbol{k}| - k_F(\omega, T) - \mathrm{Re}\Sigma(\omega))^2 + (\mathrm{Im}\Sigma(\omega))^2} \tag{5.8}$$

We can also write this as

$$\rho_B(\omega, \boldsymbol{k}) = -i\left(\frac{h_1}{|\boldsymbol{k}| - k_F(\omega) - \Sigma(\omega)} - \frac{h_1}{|\boldsymbol{k}| - k_F(\omega) - \Sigma^*(\omega)}\right) \tag{5.9}$$

Thus, using the second form, ξ is

$$\begin{aligned}\xi(\kappa) = &- \int \frac{d\omega_1}{2\pi}\frac{d\omega_2}{2\pi}\frac{f(\omega_1)-f(\omega_2)}{\omega_1-\Omega-\omega_2-i\epsilon}\frac{d^{d-1}\boldsymbol{k}}{(2\pi)^{d-1}} \\ &\times\left(\frac{h_1}{|\boldsymbol{k}+\boldsymbol{\kappa}|-k_F(\omega_1)-\Sigma(\omega_1)}-\frac{h_1}{|\boldsymbol{k}+\boldsymbol{\kappa}|-k_F(\omega_1)-\Sigma^*(\omega_1)}\right) \\ &\times\left(\frac{h_1}{|\boldsymbol{k}|-k_F(\omega_2)-\Sigma(\omega_2)}-\frac{h_1}{|\boldsymbol{k}|-k_F(\omega_2)-\Sigma^*(\omega_2)}\right)\end{aligned} \tag{5.10}$$

In the limit $\Omega \to 0$, we can combine the ω integrals into a single integral, replacing

$$\frac{f(\omega_1)-f(\omega_2)}{\omega_1-\Omega-\omega_2} \to \frac{\partial f(\omega)}{\partial\omega} = \frac{\partial}{\partial\omega}\left(\frac{1}{e^{\beta\omega}+1}\right) = -\frac{\beta e^{\beta\omega}}{(e^{\beta\omega}+1)^2} \tag{5.11}$$

and taking $\omega_1 \to \omega+\Omega$ and $\omega_2 \to \omega$. Also, we split the k integral into its angular and radial components. We find:

$$\begin{aligned}\xi(\kappa) &= \int \frac{d\omega}{2\pi}\frac{\partial f(\omega)}{\partial\omega}4h_1^2\frac{k_F^{d-2}}{(2\pi)^{d-1}}\int dk d\Omega_a \\ &\times\left(\frac{1}{k+|\boldsymbol{\kappa}|\cos\theta-k_F(\omega+\Omega)-\Sigma(\omega+\Omega)}-\frac{1}{k+|\boldsymbol{\kappa}|\cos\theta-k_F(\omega+\Omega)-\Sigma^*(\omega+\Omega)}\right) \\ &\times\left(\frac{1}{k-k_F(\omega)-\Sigma(\omega)}-\frac{1}{k-k_F(\omega)-\Sigma^*(\omega)}\right) \\ &= \int \frac{d\omega}{2\pi}\frac{\partial f(\omega)}{\partial\omega}4h_1^2 v_F\frac{k_F^{d-2}}{(2\pi)^{d-1}}\int dk d\Omega_a \\ &\times\left(\frac{1}{\omega+\Omega-v_F(k+|\boldsymbol{\kappa}|\cos\theta-k_F)+v_F\Sigma^*(\omega+\Omega)}\right. \\ &\times\left.-\frac{1}{\omega+\Omega-v_F(k+|\boldsymbol{\kappa}|\cos\theta-k_F)+v_F\Sigma(\omega+\Omega)}\right) \\ &\times\left(\frac{1}{\omega-v_F(k-k_F)+v_F\Sigma^*(\omega)}-\frac{1}{\omega-v_F(k-k_F)+v_F\Sigma(\omega)}\right)\end{aligned} \tag{5.12}$$

The factor k_F^{d-2} outside the integral assumes that $\mathrm{Re}\Sigma$ is small compared to the Fermi momentum. Note that here $d\Omega_a$ is *not* a frequency, but refers to the integration over the angular phase space of the vectors k and κ. Also, θ is the angle between the two.

We can perform the k integral by multiplying out the parentheses and applying standard contour integration to each individual term. Only two of the terms con-

tribute, since only products with one pole on each side of the real axis have non-zero contour integrals. We get:

$$\xi(\kappa) = \int \frac{d\omega}{2\pi} \frac{\partial f(\omega)}{\partial \omega} 4\pi h_1^2 \frac{k_F^{d-2}}{(2\pi)^{d-1}} \int d\Omega_a \mathrm{Im} \left(\frac{1}{|\boldsymbol{\kappa}| \cos\theta - \frac{\Omega}{v_F} + \Sigma^*(\omega + \Omega) - \Sigma(\omega)} \right) \tag{5.13}$$

Thus, the poles of the Green's function corresponding to zero sound modes in the bulk are given by the equation $1 - \xi(\kappa)\chi = 0$, where $\xi(\kappa)$ is given by 5.13 and χ by 5.3.

Chapter 6

Conclusion

We have demonstrated that quite general AdS/CFT theories possess zero sound waves in the bulk fermionic species which correspond to stable propagating excitations in the *gauge field* correlators of the boundary theory. We have explicitly calculated the poles corresponding to these waves in the case of a constant $\lambda\psi^4$ vertex - more general interactions will lead to similar, if more complicated, results. We motivated these findings by performing an analogous calculation in flat space, and see that the zero sound waves produced follow a similar form, with the exact coefficients in the AdS case determined by an effective vertex which represents an integration over the radial direction.

Thus, zero sound poles such as the ones we have described will be present in a wide variety of non-Fermi liquids and other systems described by the AdS/CFT correspondence, since they require only a general two particle scattering interaction among the fermions of their bulk description. It would be interesting to study these excitations in specific examples of non-Fermi liquids, to determine their physical manifestation and potential consequences. Zero sound waves in ordinary Fermi liquids have quite interesting and unique properties due to their propagation by deformation of the Fermi surface, and it is quite intriguing that systems can manifest this same behavior even in the absence of the quasiparticles in terms of whose interaction it was originally formulated. While materials of physical interest would no doubt have interactions more complicated the simple 4-vertex described here, a careful analysis of

the analogous processes could definitely produce useful results. Such a study could have consequences both for our understanding of general non-Fermi liquids and the high energy plasmas produced at colliders like RHIC and the LHC.

Bibliography

[1] T. Faulkner, N. Iqbal, H. Liu, J. McGreevy, D. Vegh. *Charge transport by holographic Fermi surfaces.*

[2] A. A. Abrikosov, L. P. Gorkov, I. E. Dzyaloshinski. Institute for Physical Problems, Prentice-Hall (1963)

[3] J. M. Maldacena. *The large N limit of superconformal field theories and supergravity.* Adv. Theor. Math. Phys. 2, 231 (1998). arXiv:hep-th/9711200

[4] S. S. Gubser, I. R. Klebanov and A. M. Polyakov. *Gauge theory correlators from non-critical string theory.* Phys. Lett. B 428, 105 (1998). arXiv:hep-th/9802109

[5] E. Witten. *Anti-de Sitter space and holography.* Adv. Theor. Math. Phys. 2, 253 (1998). arXiv:hep-th/9802150

[6] S. A. Hartnoll. *Lectures on holographic methods for condensed matter physics.* arXiv:0903.3246

[7] J. McGreevy. *Holographic Duality with a View Toward Many-Body Physics.* arXiv:0909.0518

[8] E. D'Hoker, D. Z. Freedman. *Supersymmetric Gauge Theories and the AdS/CFT Correspondence.* arXiv:hep-th/0201253v2

[9] C. M. Varma, Z. Nussinov, W. van Saarloos. *Singular Fermi liquids.* Phys. Rep. vol. 361, 267-417 (2002). arXiv:cond-mat/0103393

[10] G. R. Stewart. Rev. Mod. Phys. 73, 797 (2001); Rev. Mod. Phys. 79, 743 (2006).

[11] C. M. Varma, P. B. Littlewood, S. Schmitt-Rink, E. Abrahams and A. E. Ruckenstein, Phys. Rev. Lett. 63, 1996 (1989)

[12] T. Senthil. *Critical fermi surfaces and non-Fermi liquid metals.* Phys. Rev. B 78, 035103 (2008). arXiv:0803.4009 [cond-mat].

[13] T. Senthil. *Theory of a continuous Mott transition in two dimensions.* Phys. Rev. B 78, 045109 (2008). arxiv:0804.1555 [cond-mat].

[14] S. S. Lee. *A Non-fermi Liquid from a Charged Black Hole: A Critical Fermi Ball.* arXiv:0809.3402[hep-th]

[15] H. Liu, J. McGreevy, D. Vegh. *Non-Fermi Liquids from holography.* arXiv:0903.2477[hep-th]

[16] P. Coleman. *Introduction to Many Body Physics.* Rutgers University (2004)

[17] L. D. Landau. *Oscillations in a Fermi liquid.* Zh. Eksp. Teor. Fiz. 32, 59 (1957)[Soviet Phys. - JETP 5, 101 (1959)].

[18] J. de Boer. *Introduction to the AdS/CFT Correspondence.* Inst. voor Theor. Fys. Plenary Lectures (2002)

[19] J. Bekenstein, Phys. Rev. D7, 2333 (1973); Phys. Rev. D9, 3293 (1974); S. W. Hawking, Phys. Rev. D13, 191 (1976).

[20] L. Susskind. *The World as a Hologram.* Journal of Mathematical Physics 36 (11):6377-6396 (1995). arXiv:hep-th/9409089